iJRASET
International Journal For Research in Applied Science and Engineering Technology



INTERNATIONAL JOURNAL FOR RESEARCH

IN APPLIED SCIENCE & ENGINEERING TECHNOLOGY

Volume: 11 **Issue:** IV **Month of publication:** April 2023

DOI: https://doi.org/10.22214/ijraset.2023.50753

www.ijraset.com

Call: 08813907089 | E-mail ID: ijraset@gmail.com

International Journal for Research in Applied Science & Engineering Technology (IJRASET)
ISSN: 2321-9653; IC Value: 45.98; SJ Impact Factor: 7.538
Volume 11 Issue IV Apr 2023- Available at www.ijraset.com

Design of Multilevel Inverter based Active Filter for Harmonic Elimination & Frequency Regulation

Shubhang Bandyopadhyay[1], Tathagata Rout[2], Harsh Vardhan Rathi[3]
Vellore Institute of Technology, Chennai

Abstract: ***For harmonic and reactive power adjustment in two-wire (single phase), three-wire (three phase without neutral), and four-wire (three phase with neutral) ac power networks with nonlinear loads, active filtering of electric power has already reached maturity.***
This article provides a thorough analysis of active filter (AF) designs, control methods, component choices, additional relevant technical and economic factors, and their selection for certain applications. It aims to give researchers and application developers working with AF technology a comprehensive perspective on the state of the technology.
Keywords: Active power filters, Control algorithms, Current controllers, Comparison, Harmonic currents Power quality, Total harmonic distortion, Root mean square (RMS) error.

I. INTRODUCTION

Power engineers encounter issues with power quality when nonlinear harmonic generating loads are used in the distribution system. Because of developments in semiconductor technology, power electronics devices are being used by end users much more frequently. Problems like harmonic production, poor power factor, reactive power disturbance, low system efficiency, disruption to other consumers, device heating, etc. are brought on using power electronics devices. It is crucial to minimise this issue because it may grow significantly in the coming year.

APFs are frequently employed in power systems to reduce harmonic distortion. They introduce harmonic components into the electrical network via power electronics converters that counteract the harmonics introduced by non-linear loads in the source currents.

Lower order harmonics of the line current (5th, 7th, 11th, etc.) have been eliminated using passive LC filters, which have also been employed to control the flow of harmonic currents in the distribution system. However, these passive second order filters have a few drawbacks, including series and parallel resonances, tuning issues, and power system complexity, especially when there are more harmonic elements that must be suppressed.

II. ACTIVE POWER FILTERS

In the past thirty years, active filters have been created, enhanced, and commercialised. They can be used to correct current-based distortions such neutral current, reactive power, and current harmonics. They are also used to correct voltage-based distortions such voltage harmonics, flickering, sags, and imbalances[1].

There are two types of active filters: single-phase and three-phase. Single phase active filters are used to compensate for power quality problems caused by single-phase loads such as DC power supplies. Three-phase active filters can have or not have a neutral connection. Three-phase active filters are used for high-power nonlinear loads like adjustable speed drives (ASDs) and AC-to-DC converters [1], [3].

There are two types of active filters based on topologies: current source active filters and voltage source active filters. As shown in Fig. 1, current source active filters (CSAF) use an inductor as the DC energy storage device. As shown in Fig. 2, a capacitor serves as the storage element in a voltage source active filter (VSAF). In comparison to CSAF, VSAF are less expensive, lighter, and easier to control [1], [3]. Active filters can be connected in a variety of ways, including shunt active filters, series active filters, parallel active filters, and hybrid active filters [3].

A shunt active filter can remove harmonics from commercial and industrial power supplies. Simon Round and colleagues use a new technique based on sinusoidal subtraction to create an inverter that is more responsive to harmonics [4].

©IJRASET: All Rights are Reserved

ISSN: 2321-9653; IC Value: 45.98; SJ Impact Factor: 7.538
Volume 11 Issue IV Apr 2023- Available at www.ijraset.com

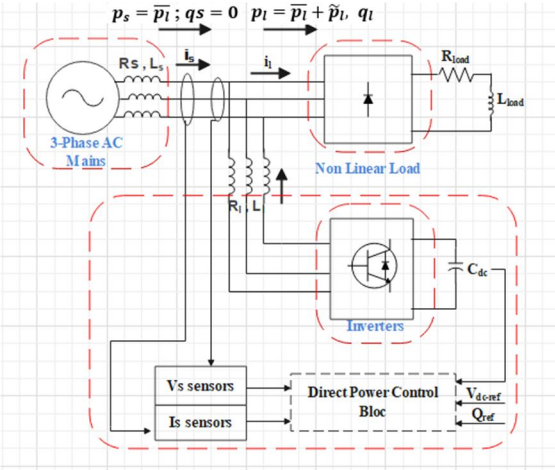


Figure 1: Active Shunt Filter

III. COMPENSATION METHODOLOGY

The idea of using this active design, as shown in Fig. 1, is to account for reactive power and reduce harmonic components. The active filter can be used as a controlled source of current to generate a current wave that is as near to the current reference as feasible. A balance between instantaneous power supplied by the source and the active filter and drained by the load must be determined to generate the current reference. If ps and qs are the main's real and imaginary instantaneous powers, and pf and qf are the active power filter's real and imaginary instantaneous powers, then the main ought to provide ps=pl and qs=0 to offset reactive energy and minimize harmonic currents. To accomplish power compensation, the APF must serve the oscillatory component of pl, whereas ql must be completely supplied by the APF. Because the oscillating component of **pl** is due to harmonic components, when it is sent to the load by the active filter, the source current remains sinusoidal while the load continues to receive the same amount of harmonic and fundamental current. Power balance results in:

$$p_s = \overline{p_l} \; ; qs = 0$$
$$p_f = p_l - p_s = \overline{p_l} + \tilde{p}_l - \overline{p}_l \qquad (1)$$
$$q_f = q_l - q_s = q_l \qquad (2)$$

To account for the functions . these functions of the capacitor mostly on inverter's DC side, earlier Eqs.(1) and (2) must be revised. The capacitor stores energy that is utilised to power the active filter during normal conditions. In an ideal world, APF does not feed active power in normal operation because it should be able to supply $p_f = \tilde{p}_l$, $q_f = q_l$ and hence just reactive power. As a result, the capacitor voltage level is constant in steady state and changes during transients. Voltage value management is required to regulate voltage level in steady state and to limit voltage variability during transients and startup. As a result, the computation of the current reference wave should take into account the necessity to shift power balance in order to charge or discharge the active filter's DC side capacitor.

It is important to control active power balance among source, load, and APF in order to adjust DC voltage level. When the load consumes a particular power consumption $\overline{p_l}$ and $p_s > \overline{p_l}$, the APF draws extra power, enhancing DC side voltage. Because the load demands a specific amount of power, if **ps pl**, the APF pumps the remaining fraction such that $\overline{p}_s + \overline{p}_f = \overline{p}_l$ and so the DC bus voltage level drops.

IV. HYSTERESIS-BAND CURRENT CONTROL

This technique produces a hysteresis band in which the actual current continuously tracks the command current. Figure 2 depicts the HCC for a single phase VSI. Assume that a sinusoidal voltage source e is connected to the VSI terminal voltage u via an equivalent inductance **L** and resistance **R**. If a certain reference current, $\mathbf{I_r}$, needs to be monitored, the APF output current can be regulated. The retrieved error signal is compared against present upper and lower tolerance limits. If the fault is within the tolerance zone, no switching occurs. Switching occurs when an error surpasses the tolerance balance.

©IJRASET: All Rights are Reserved

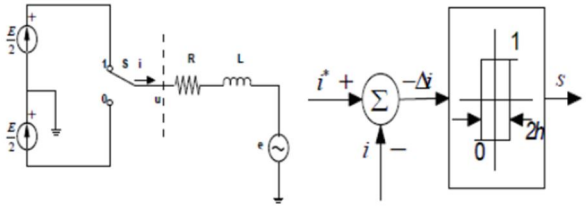


Figure 2: Hysteresis Controller

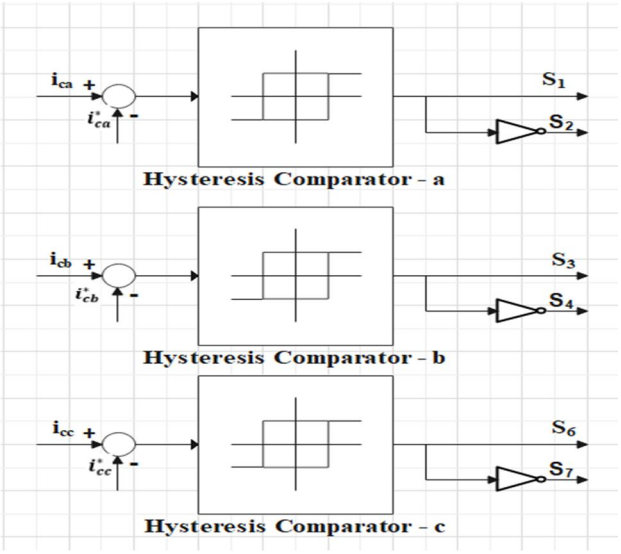


Figure 3: Pulse generation using hysteresis current control technique

V. INSTANTANEOUS REACTIVE POWER THEORY

Akagi et al. proposed the p-q theory in 1983. The p-q theory is based on converting a-b-c coordinates to -0 coordinates and —0 coordinates to a-b-c coordinates, also known as Clark transformation and inverse transformation. Fig. 4 depicts a basic block diagram of p-q theory. The compensatory current generated will be:

$$I_{comp} = I_{source} - I_{load} \quad (3)$$

Where,

$\mathbf{I_{comp}}$ = Compensating Current
$\mathbf{I_{source}}$ = Source Current
$\mathbf{I_{load}}$ = Load Current

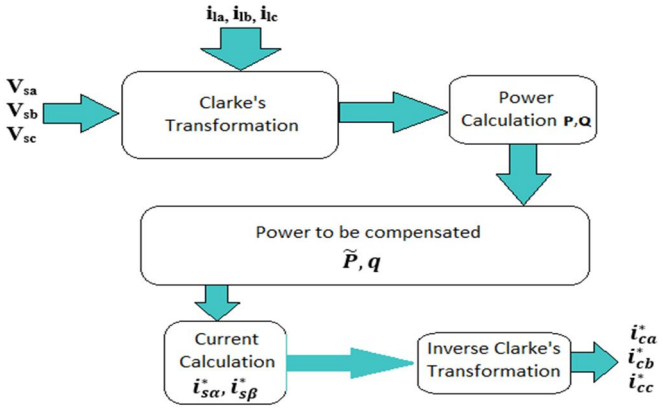


Figure 4: Block Diagram P-Q theory

This method transforms 3-phase source voltage and load current into a fixed reference frame with $\boldsymbol{\alpha - \beta - 0}$ phase angle.

$$\begin{bmatrix} V_0 \\ V_\alpha \\ V_\beta \end{bmatrix} = \sqrt{\frac{3}{2}} \begin{bmatrix} \frac{1}{\sqrt{2}} & \frac{1}{\sqrt{2}} & \frac{1}{\sqrt{2}} \\ 1 & \frac{1}{2} & -\frac{1}{2} \\ 0 & \frac{\sqrt{3}}{2} & -\frac{\sqrt{3}}{2} \end{bmatrix} \begin{bmatrix} V_{sa} \\ V_{sb} \\ V_{sc} \end{bmatrix} \quad \textbf{(4)}$$

$$\begin{bmatrix} I_0 \\ I_\alpha \\ I_\beta \end{bmatrix} = \sqrt{\frac{3}{2}} \begin{bmatrix} \frac{1}{\sqrt{2}} & \frac{1}{\sqrt{2}} & \frac{1}{\sqrt{2}} \\ 1 & \frac{1}{2} & -\frac{1}{2} \\ 0 & \frac{\sqrt{3}}{2} & -\frac{\sqrt{3}}{2} \end{bmatrix} \begin{bmatrix} I_{sa} \\ I_{sb} \\ I_{sc} \end{bmatrix} \quad \textbf{(5)}$$

These updated figures are used to calculate the load's instantaneous real and reactive power, which consists of a mean and an oscillating component.

$$\begin{bmatrix} P_0 \\ P \\ q \end{bmatrix} = \begin{bmatrix} V_0 & 0 & 0 \\ 0 & V_\alpha & V_\beta \\ 0 & -V_\beta & V_\alpha \end{bmatrix} \begin{bmatrix} I_0 \\ I_\alpha \\ I_\beta \end{bmatrix} \quad \textbf{(6)}$$

In three phase three wire systems, $I_0 = 0$, hence source power $P_0 = 0$. As a result, the power equation becomes as follows.

$$\begin{bmatrix} P \\ q \end{bmatrix} = \begin{bmatrix} V_\alpha & V_\beta \\ -V_\beta & V_\alpha \end{bmatrix} \begin{bmatrix} I_\alpha \\ I_\beta \end{bmatrix} \quad \textbf{(7)}$$

The load's instantaneous active and reactive power can be computed as follows:

$$\begin{bmatrix} P_l \\ q_l \end{bmatrix} = \begin{bmatrix} V_\alpha & V_\beta \\ -V_\beta & V_\alpha \end{bmatrix} \begin{bmatrix} I_{l\alpha} \\ I_{l\beta} \end{bmatrix} \quad \textbf{(8)}$$

Instantaneous real and reactive power can be divided into two parts: oscillatory components and average components. When the main supply is perfectly balanced and sinusoidal, the mean power component represents the positive sequence's first harmonic current, and the oscillatory components are connected to all high order harmonic components, including the negative sequence's first harmonic current. As a result, the oscillatory power components must be rectified by the shunt active filter, resulting in the same average power components in the main supply.

$$\begin{bmatrix} I_{s\alpha} \\ I_{s\beta} \end{bmatrix} = \frac{1}{V_\alpha^2 + V_\beta^2} \begin{bmatrix} V_\alpha & -V_\beta \\ V_\beta & V_\alpha \end{bmatrix} \begin{bmatrix} \overline{p} \\ 0 \end{bmatrix} \quad \textbf{(9)}$$

A high-pass filter helps eliminate the oscillating component, and compensating reference signals in terms of currents or voltages are created by taking the inverse of-transformation α-β transformation.

$$\begin{bmatrix} I_{ca}^* \\ I_{cb}^* \\ I_{cc}^* \end{bmatrix} = \sqrt{\frac{2}{3}} \begin{bmatrix} 1 & 0 \\ -\frac{1}{2} & \frac{\sqrt{3}}{2} \\ -\frac{1}{2} & -\frac{\sqrt{3}}{2} \end{bmatrix} \quad \textbf{(10)}$$

VI. PERFORMANCE ANALYSIS

[MATLAB SimPowerSystem tools are used to create a simulation model of a five-level MLI-based APF. Extensive simulation studies are conducted to investigate the performance of the APF during transients as well as steady states for various loading conditions. Several performance characteristics, such as THD and reactive power correction, are provided before and after compensation.]

1) Case 1: Linear Loads

The diagrams represented in Fig 5 and Fig 6 shows that the three-phase voltage source is connected to the two linear loads i.e., resistive, and inductive via shunt active filter. The two scenarios of each of the linear loads have been taken into account and analyzed accordingly using the Simulink model. In the diagram Fig 5, two resistive loads are connected with and without a switch to the three-phase voltage source via shunt active filter. The switching time is 0.17s. Same as Fig 5, two inductive loads with and without a switch are connected in Fig 6. The Simulink model will undergo FFT Analysis and generate the rate of total harmonic distortion in each case, from where we can infer the performance of the shunt active filter in each load.

V_s = 4160 V	f = 50Hz	P_R = 1000 W
$L_s = 10^5$	R_s = 0.1 Ω	T_s = 0.25 secs

Table 1: Simulation Parameters

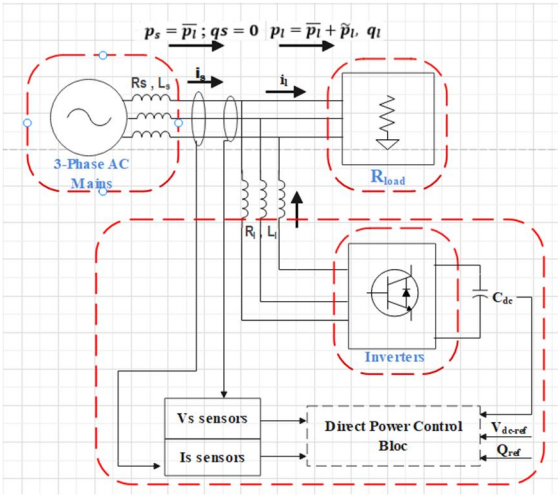


Figure 5: Circuit with Resistive Load

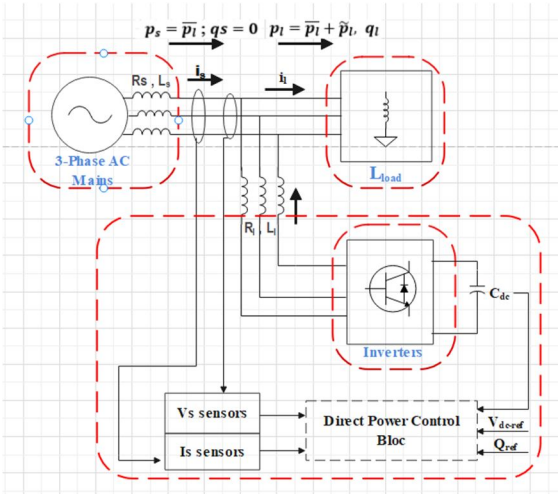


Figure 6: Circuit with Inductive Load

2) Case 2: Non-Linear Load

Fig. 11 represents a circuit of Non-linear load in the form of diodes. We replace the linear R or L loads with diodes connected in the form of a three-phase rectifier.

V_s = 4160 V	**f = 50Hz**

Table 2: Parameters of Non-Linear load

In the diagram Fig 8, two non-linear loads are connected with and without a switch to the three-phase voltage source via shunt active filter. The switching time is 0.17s. The Simulink model will undergo FFT Analysis and generate the total harmonic distortion (**THD**) in each case, from where we can infer the performance of the shunt active filter in each load.

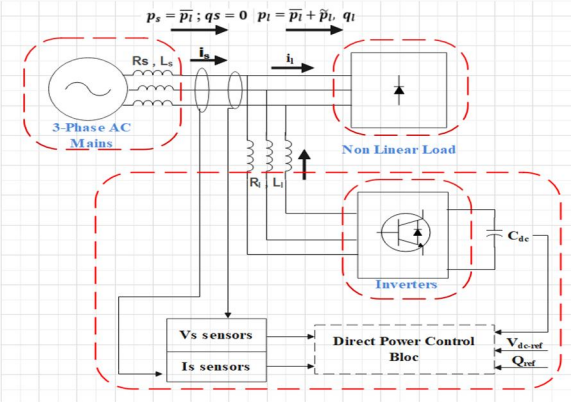


Figure 7: Circuit with Non-Linear Load

3) Case 3: With Distorted Voltage Supply

The circuit depicts a dynamic voltage supply to create harmonics from the source side while maintaining a non-linear load. A R-L Load is connected on the DC side of the rectifier.

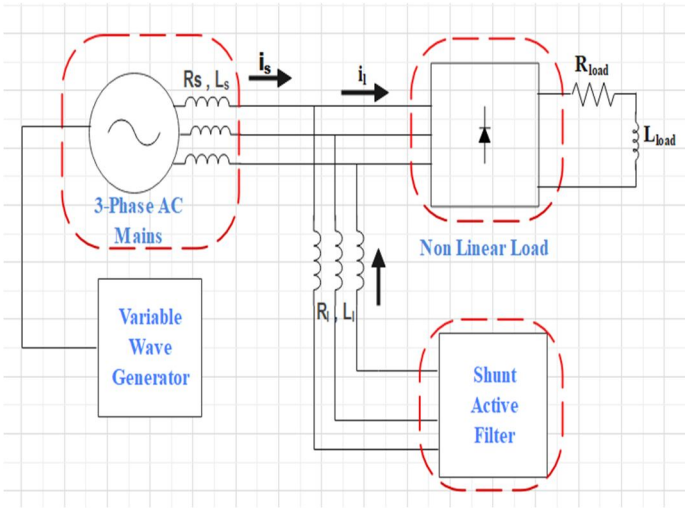


Figure 8: Circuit with Distorted Supply

4) Case 4: Phase Controlled Converter with R-L Load

While uncontrolled rectifier circuits are still widely used, for some applications, additional control and efficiency are required. This is achievable by employing a controlled rectifier circuit wherein thyristors in full-bridge configuration adjust the mean voltage. A gate on each thyristor controls when it turns on.

Yet, when the firing angle of the converter increases, the quality of the AC side power will degrade even further. At increasing firing angle and %THD, the input power factor degrades. These converters generate currents with strong rising and falling edges, complicating the APF work. The power and frequency of the distortion, which vary with firing angle, limit the usefulness of APF.A passive filter is required at the input of converter. This passive filter limits the slope of the rising and falling edges of the load currents, which makes the task of APF easy.

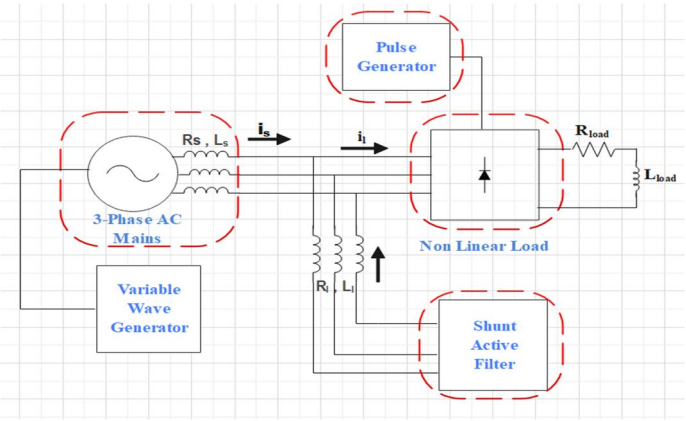


Figure 9: Circuit with firing pulse generator

VII. SIMULATIONS OBSERVED

The following graphical representations are established from observed total harmonic distortion (THD).

1) Case 1: Linear Load

In Fig 9, the THD value obtained for the resistive load without switching is 0.46%. Similarly, for inductive load in Fig 10, the THD value obtained is 0.52%. But when there is a load switching at t=0.25secs, there is a sharp increase in THD value for both resistive and inductive load i.e., 290.77% and 68.39% respectively (see Fig 9 and Fig 10).

Due to load switching at a finite time, a disturbance is created in the switching side of the load for a continuous ON and OFF situation which results in an increase in THD value.

The switch however creates a disturbance leading to an increment in THD.

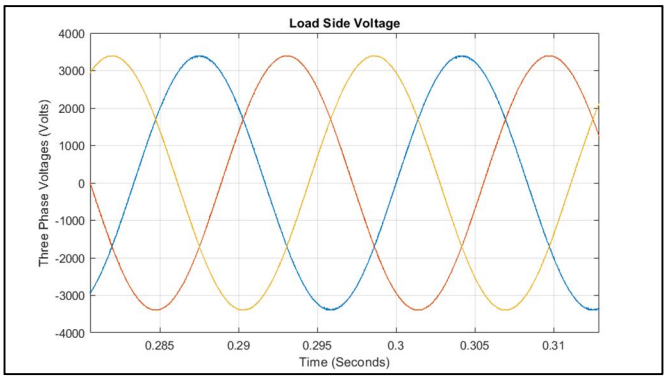


Figure 10: Load Voltage R-Load and L-Load

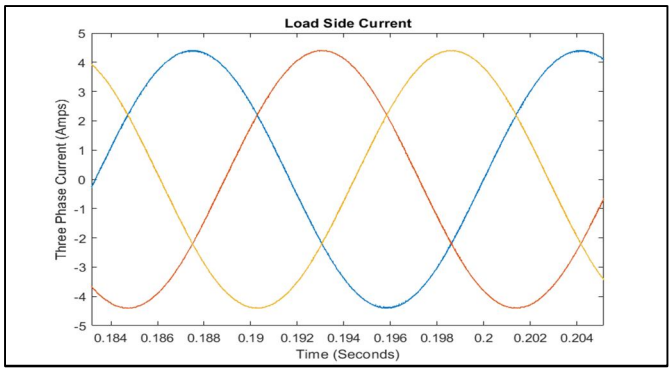


Figure 11: Load Current R-Load and L-Load

Load Type	Without Switch	With Switch
Resistive	0.46 %	290.77 %
Inductive	0.52 %	292.87 %

Table 3: THD data on Linear Load

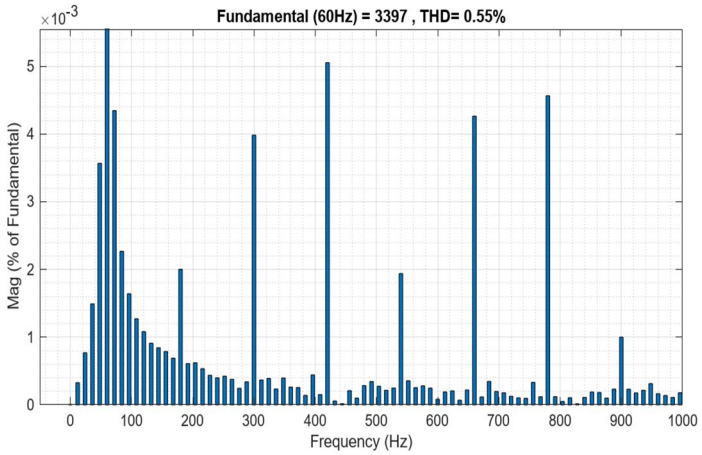


Figure 12: Resistive Load with no switch

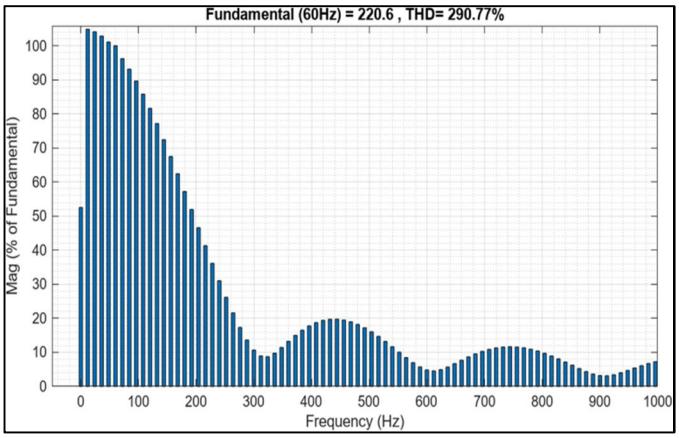


Figure 13: Resistive Load with switch

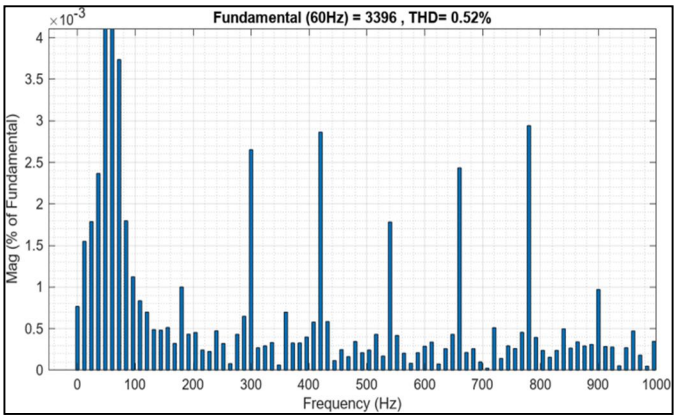


Figure 14: Inductive Load with no switch

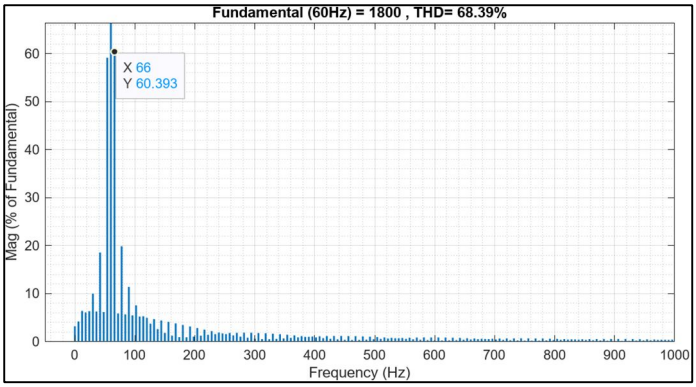


Figure 15: Inductive Load with switch

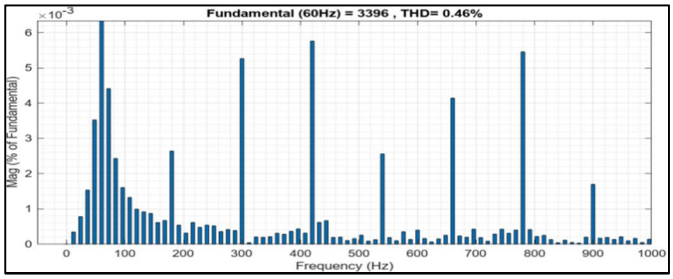


Figure 16: THD of source

2) Case 2: Non-Linear Load

Fig. 11 represents a circuit of Non-linear load in the form of diodes. When there are nonlinear loads, the current on a waveform does not appear like the voltage. Harmonics are caused by loads, therefore in this situation we have current altering the voltage. As we draw current through the system, the nonlinear load induces current distortion, which leads to voltage distortion.

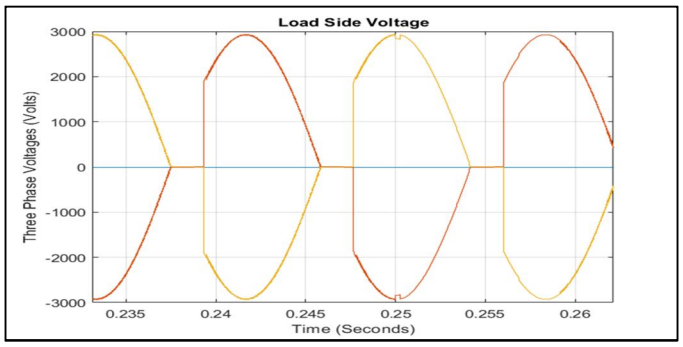


Figure 17: Load Voltage with no switch

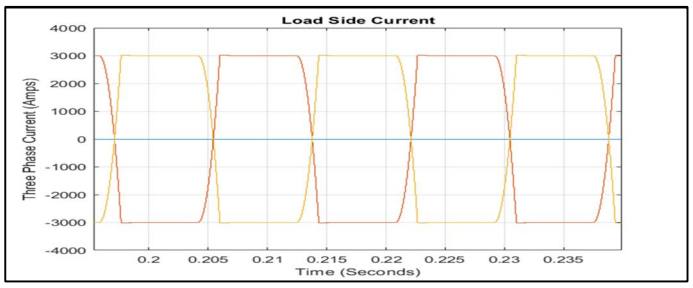


Figure 18: Load Current with no switch

Again, with linear loads, the voltage and current sine waves will be identical. Current drawn from a standard motor or light can appear to be the clean voltage, even if it is not in phase or is slightly leading or lagging—this relies on the power factor of the load. Before and after the load shift, the source current maintains sinusoidal. To accommodate for the sudden change in load current, the DC capacitor voltage strayed from its standard value. Capacitor responds to an increase in load current, rather than an instant rise in power consumption. This creates a dip in capacitor voltage, which is quickly regained. Similarly, APF responds to a decline in load current by boosting capacitor voltage and restoring power quickly.

Load Type	With No Switch	With Switch
Non-Linear (Diode)	644.01 %	71.85 %

Table 4: THD Observed

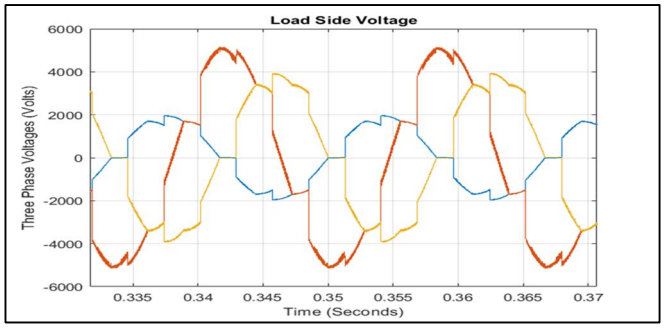


Figure 19: Load Voltage with switch

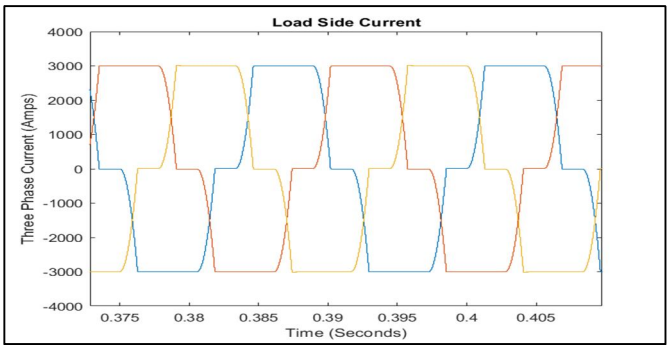


Figure 20: Load Current with switch

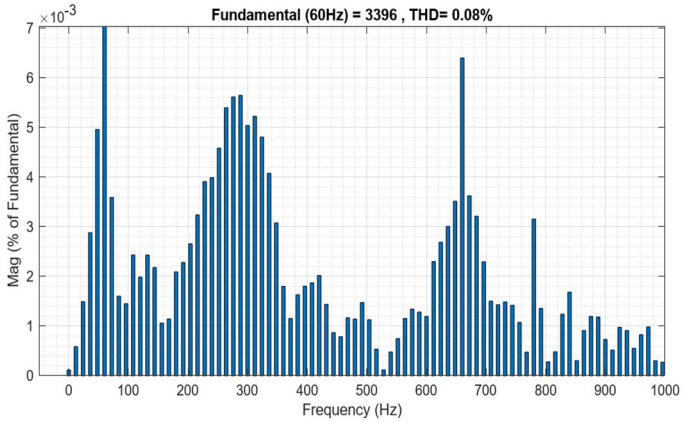


Figure 21: THD of source

3) Case 3: With distorted supply

Fig. 22 represents the source voltage having a sudden spike at instants t=0.1, 0.15, 0.2 secs. These spike results in a disrupted supply leading to harmonics.

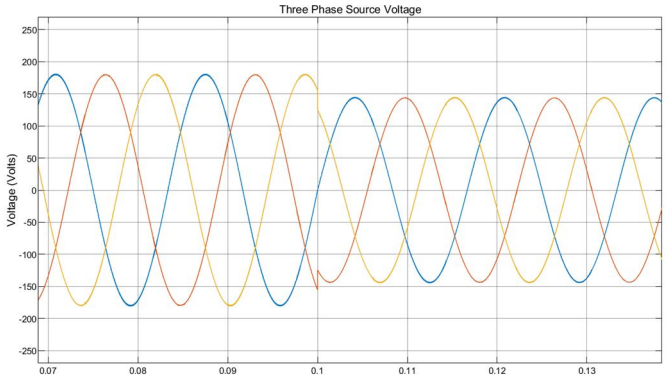


Figure 22: Source Voltage

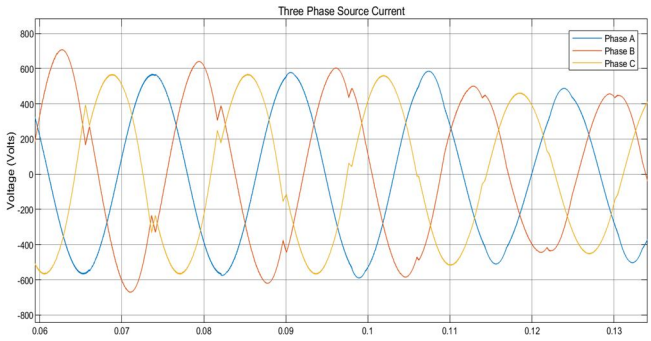


Figure 23: Source Current

The load voltage and load current follow the locus of source voltage and current even the disruption caused. This is due to linear loads present instead of non-linear loads.

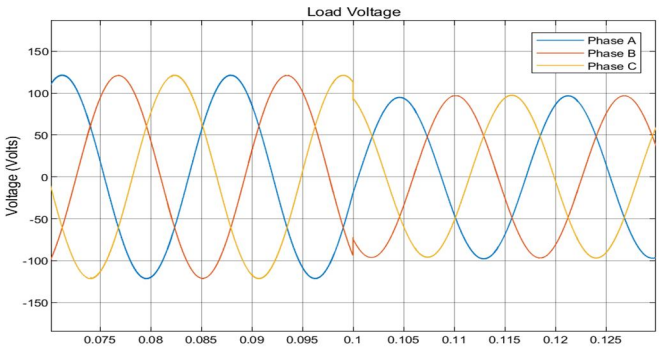


Figure 24: Load Voltage

The THD difference is starkly evident when comparing the FFT analysis with/without compensator.

	THD
With Compensator	**3.94 %**
Without Compensator	**47.14 %**

Table 5: THD comparison

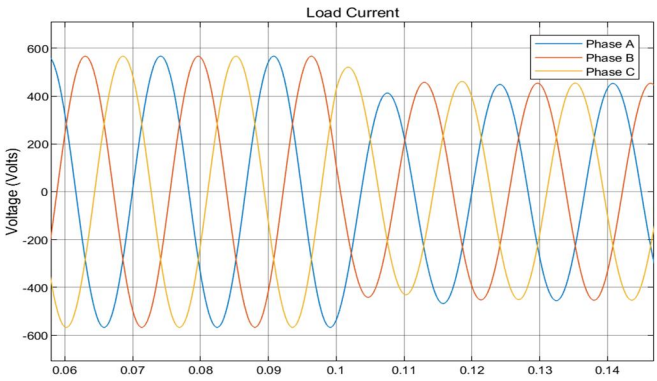


Figure 25: Load Current

The supply voltage contains seventh harmonics and THD is 47.14%. Generally distorted supply voltage causes increase in the load current THD as compared with results to ideal voltage case. Figures 22, 23, 24, and 25 illustrate the deformed input phase voltage, load current, corrected source current, and filter current waveforms for phases A, B, and C, respectively.

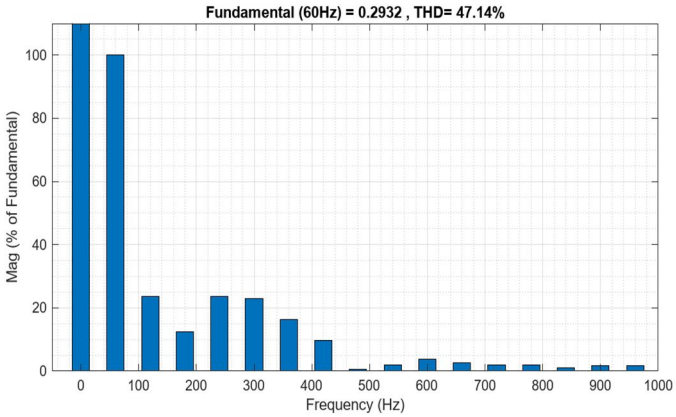


Figure 26: THD of source before compensation

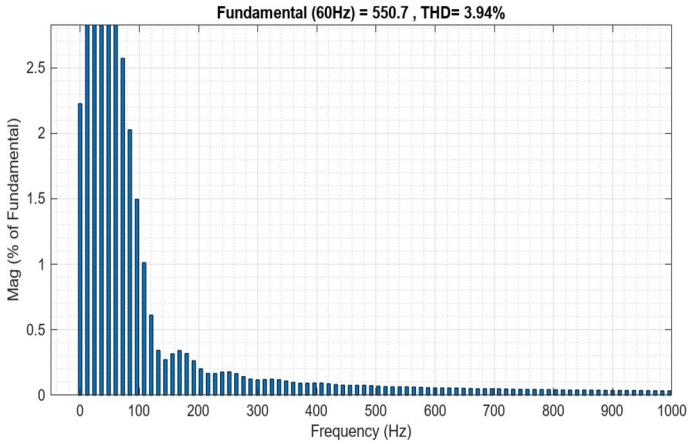


Figure 27: THD of source after compensation

4) Case 4: Phase Controlled Converter with RL-Load

The rectifier circuit's nonlinearity rises as the firing angle (**α**) increases. This means that the waveforms of the output voltage as well as the input current will be less sinusoidal in nature. As a result, the device's harmonic content is high across its input and output.

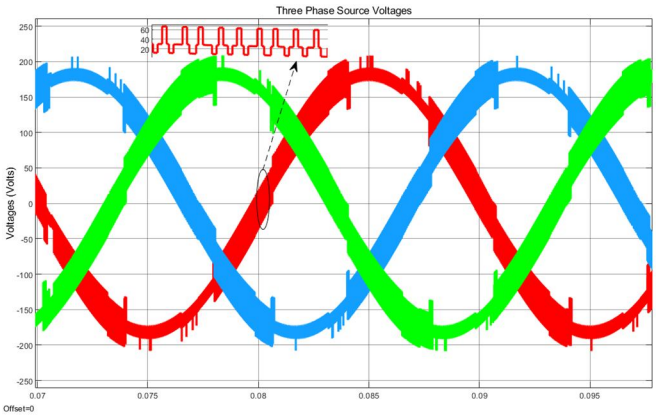


Figure 28: Source Voltage

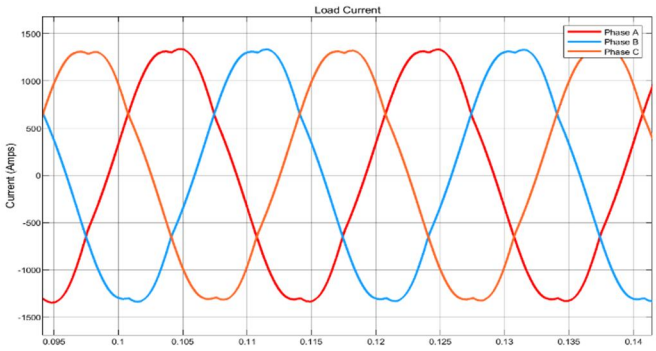


Figure 29: Source Current

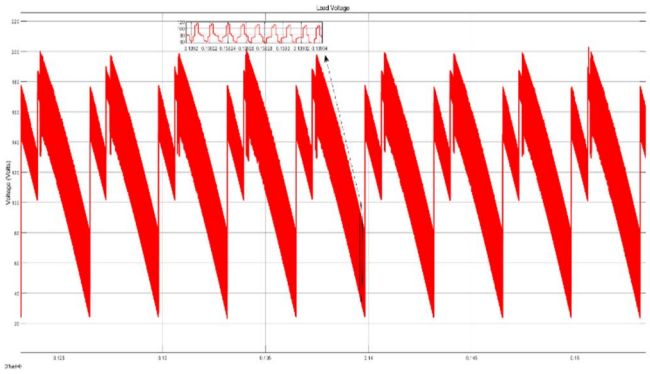


Figure 30: Load Voltage

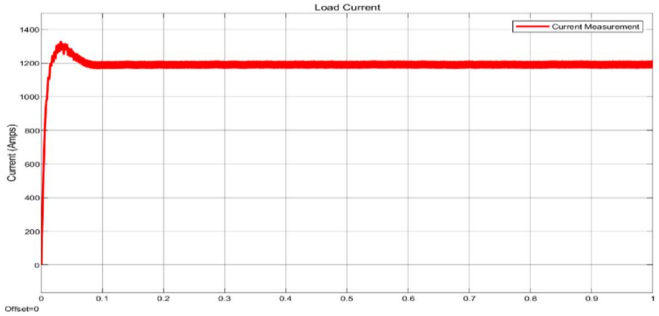


Figure 31: Load Current

At the rectifier's input, the voltage provided by the grid is basically consistent, and the device's mechanics allow the input voltage to stay sinusoidal with minimum harmonic distortion. In contrast, the conduct of the input current is dictated as to how frequently the thyristors operate inside of the rectifier.

At **α = 30°**, THD received is

At **α = 60°**, THD received is

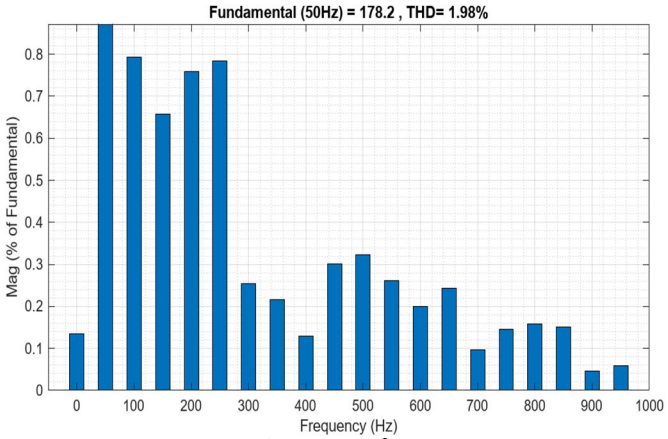


Figure 32: THD of source

Fig. 31 depicts the APF performance waveforms for a phase regulated converter as a nonlinear load at a firing angle of 30°. The displacement angle increases as the firing angle increases, resulting in increased reactive power. Furthermore, when the firing angle increases, the current commutation process shifts towards the region surrounding the peak of the line-to-line voltage, complicating the APF's duty. Figures 28, 29, 30, 31 show steady-state waveforms. Figures 32 and 33 illustrate the frequency spectrum of the source current before and after correction.

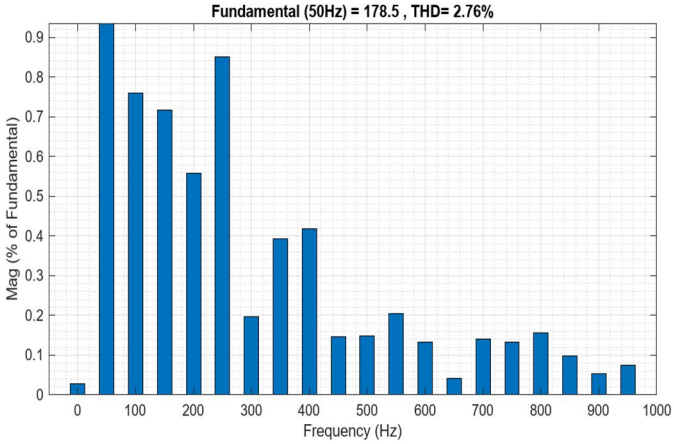


Figure 33: THD of source

Firing Angle	THD
α = 30°	1.98 %
α = 60°	2.76 %

Table 6: THD of source

VIII. CONCLUSION

A shunt APF based on MLI is researched for harmonic compensation of high-power high voltage nonlinear loads. MLI eliminates the requirement for a high-rating transformer in a high-voltage system. To generate APF reference currents, the instantaneous reactive power theory is applied. The fact that real and reactive powers associated with fundamental components are DC quantities is a benefit of p-q theory.

These values can be retrieved using a low pass filter. Gating signals are generated using carrier phase shifted PWM. Despite the converter's high frequency output, the CPS-PWM approach minimises individual device switching frequency.

Extensive simulation results are achieved to validate the APF's performance during transient and steady-state circumstances for various loading scenarios. The suggested approach successfully adjusts current harmonics of nonlinear loads in high voltage systems. After correction, the source current becomes sinusoidal and in phase with the source voltages.

The corrected source current's THD falls substantially below 5%, which is the maximum limit specified by the IEEE 519-1992 standard.

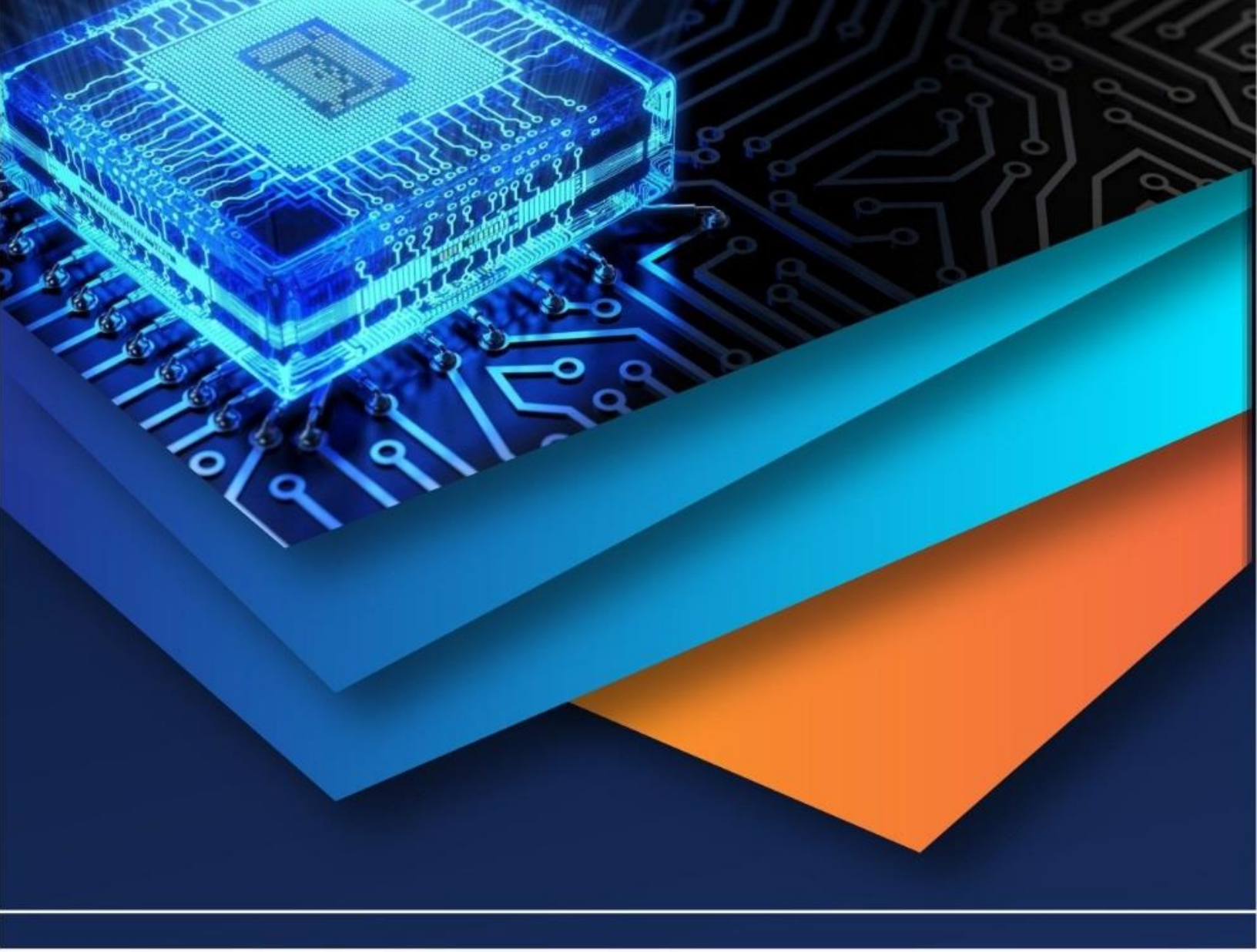
Nonlinear loads, such as diode rectifiers with R-C components and phase regulated converters, draw current with strong rising and falling edges, making APF's job more difficult. To facilitate APF operation and achieve effective compensation, a passive filter is connected in front of the nonlinear load.

The p-q theory is appropriate when supply voltages are optimal, however mains voltages in typical industrial power systems are frequently distorted. In this scenario, the p-q theory produces mistakes in reference currents and limits compensation. Even when the supply voltage is distorted and there are unbalanced loads, the average power approach produces accurate results.

In addition, the performance of a seven-level MLI-based APF is explored. When compared to five-level MLI, the DC side capacitor voltage is reduced. It demonstrates that for higher voltages, higher-level MLI can be employed to avoid the usage of a costly and bulky transformer.

REFERENCES

[1] Emadi, A. Nasiri, and S. B. Bekiarov, “Uninterruptible Power Supplies and Active Filter”, Florida, 2005, pp. 65-111.
[2] D. W. Hart, “Introduction to Power Electronics”, New Jersey, 1997, pp. 291-335.
[3] M. McGranaghan, “Active Filter Design and Specification for Control of Harmonics in Industrial and Commercial Facilities”, 2001.
[4] S. Round, H. Laird and R. Duke, “An Improved Three-Level Shunt Active Filter”, 2000.
[5] H. Lev-Ari, “Hilbert Space Techniques for Modeling and Compensation of Reactive Power in Energy Processing Systems”, 2003.
[6] A. Emadi, “Modeling of Power Electronic Loads in AC Distribution Systems Using the Generalized State-Space Averaging Method”, 2001. [7] P.T Krein, J. Bentsman, R. M. Bass, B. C. Lesieutre, “On the Use of Averaging for Analysis of Power Electronic System”, 1990.
[7] F. Kamran, “A Novel On-Line UPS with Universal Filtering Capabilities”, 1998.
[8] Mark McGranaghan, “Active Filter Design and Specification for Control of Harmonics in Industrial and Commercial Facilities”, Electrotek Concepts, Inc. 2002.
[9] Mika Salo and Heikki Tuusa, “A novel OpenLoop Control Method for a Current–Source Active Power Filter”, IEEE Trans on Industrial Electronics, Vol. 50, No. 2, April 2003.
[10] Moleykutty George and Kartik Prasad Basu, “Three-Phase Active Power Filter”, 2008.
[11] R. Pregitez, J.G. Pinto, Luis F. C. Monteiro and Joao L. Afonso, “Shunt Active Filter with Dynamic Output Current Limitation”, 2007.
[12] Eswaran Chandra Sekaran, Ponna Nadar Anbalang and Chelliah Palanisamy, “Analysis and Simulation of a New Shunt Active Power Filter using Cascaded Multilevel Inverter”, 2007.
[13] Moleykutty George and Kartik Prasad Basu, “Modeling and Control of Three-Phase Shunt Active Power Filter”, 2008.
[14] I. Zamora, P. Eguia, A. J. Mazon, E. Torres and K. J. Sagasteita, “Using Active Filters to reduce THD in Traction System”.
[15] Hanny H. Tumbelaka, Lawerance J. Borle, “A Grid Current-controlling Shunt Active Power Filter”, 2007.
[16] Luiz Moran, Marcelo Daiz, Victor Higuera, Rogel Wallace and Juan Dixon, “A Three-Phase Active Filter Operation with Fixed Switching Frequency for Reactive Power and Current Harmonic Compensation".
[17] Zhong Du, Leon M. Tolbert and John N. Chiasson, “Active Harmonic Elimination for Multilevel Converter”, 2006.
[18] M.C.Ben Habib, E. Jacquot and S. Saadate, “An Advanced Control Approach for a Shunt Active Power Filter”.
[19] A. D. Le Roux, J. A du Toit and J.H.R Enslin, “Integrated Active Reactive and Power Quality Compensator with Reduced Current Measurement”, 1999.



10.22214/IJRASET

45.98

IMPACT FACTOR: 7.129

IMPACT FACTOR: 7.429

INTERNATIONAL JOURNAL FOR RESEARCH

IN APPLIED SCIENCE & ENGINEERING TECHNOLOGY

Call : 08813907089 (24*7 Support on Whatsapp)